

# Evaluation of In-situ observations on Marine Weather Observer during the Typhoon Sinlaku

Wenyang He<sup>1,2</sup>, Hongbin Chen<sup>1,2</sup>, Hongyong Yu<sup>3</sup>, Jun Li<sup>1</sup>, Jidong Pan<sup>1</sup>, Shuqing Ma<sup>4</sup>,  
Xuefen Zhang<sup>4</sup>, Rang Guo<sup>4</sup>, Bingke, Zhao<sup>5</sup>, Xi Chen<sup>6</sup>, Xiangao Xia<sup>1,2</sup>, Kaicun Wang<sup>7</sup>

<sup>1</sup>Key Laboratory of Middle Atmosphere and Global Environment Observation, Institute of Atmospheric Physics, Chinese Academy of Sciences, Beijing 100029, China

<sup>2</sup>School of the Earth Science, Chinese Academy of Science University, Beijing 100049, China

<sup>3</sup>State Key Laboratory of Earth Surface Processes and Resource Ecology, College of Global Change and Earth System Science, Beijing Normal University, Beijing, China

<sup>4</sup>Meteorological Observation Center of the China Meteorological Administration, Beijing 10081, China

<sup>5</sup>Shanghai Typhoon Institute of CMA, Shanghai 200030, China;

<sup>6</sup>Shanghai Marine Meteorology Center, Shanghai Meteorology Center, Shanghai 200030, China;

<sup>7</sup>Peking University, Beijing 100029, China

**Correspondence:** Wenyang He (hwy@mail.iap.ac.cn) and Hongbin Chen (chb@mail.iap.ac.cn)

## Abstract

The mobile ocean weather observation system, named Marine Weather Observer (MWO), developed by the Institute of Atmospheric Physics (IAP), consists of a fully solar-powered, unmanned vehicle and meteorological and hydrological instruments. One of the MWOs completed a long-term continuous observation, actively approaching the Typhoon Sinlaku center from July 24 to August 2, 2020, over the South China Sea. The in-situ and high temporal resolution(1-min) observations obtained from MWO were analyzed and evaluated by comparing with the observations made by two types of buoys during the evolution of Typhoon Sinlaku. First, the air pressure and wind speed measured by MWO are in good agreement with those measured by the buoys before the typhoon, reflecting the equivalent measurement capabilities of the two methods under normal sea conditions. The sea surface

31 temperature (SST) between MWO and the mooring buoys is highly consistent  
32 throughout the observation period, indicating the high stability and accuracy of SST  
33 measurements from MWO during the typhoon evolution. The air temperature and  
34 relative humidity measured by MWO have significant diurnal variations, generally  
35 lower than those measured by the buoys, which may be related to the mounting height  
36 and sensitivity of sensors. When actively approaching the typhoon center, the air  
37 pressure from MWO can reflect some drastic and subtle changes, such as a sudden  
38 drop to 980 hPa, which is difficult to obtain by other observation methods. As a  
39 mobile meteorological and oceanographic observation station, MWO has shown its  
40 unique advantages over traditional observation methods, and the results preliminary  
41 demonstrate the reliable observation capability of MWO in this paper.

42

## 43 **1 Introduction**

44 Marine meteorological hazards, including typhoons, fog, strong winds, and many  
45 other extreme weather events, occur frequently over China (Xu et al., 2009). In  
46 particular, typhoons that make landfall off the southeast coast of China cause direct  
47 economic losses of about 0.4% of gross domestic product and more than 500 deaths  
48 per year (Lei, 2020). Many efforts have been made in recent decades to improve the  
49 understanding of typhoon genesis and evolution and the forecasting of typhoon paths  
50 (Bender et al. 2007; Black et al. 2007; Sanford et al. 2007; Bell et al. 2012). However,  
51 errors in model initial conditions remain the main cause of typhoon forecast  
52 uncertainty due to the scarcity of real-time ocean meteorological observations,

53 especially in distant waters (Zheng et al. 2008; Rogers et al. 2013; Emanuel and  
54 Center 2018). Currently, marine observations over China are very limited and rarely  
55 occur in the deep ocean (Dai et al., 2014). This situation greatly limits the  
56 development of marine meteorology, especially the improvement of typhoon  
57 forecasting. Therefore, there is a urgent need to develop advanced observation  
58 techniques at sea. With the rapid development of satellite communication and  
59 navigation technology as well as sensor technologies in recent years, marine  
60 unmanned autonomous observation systems have been increasingly broken and  
61 applied at sea (Lenan and Melville, 2014; Wynn et al., 2014; Thomson and Girton,  
62 2017).

63 To obtain more meteorological observations at sea, the Institute of Atmospheric  
64 Physics (IAP), Chinese Academy of Sciences, has developed an automatic and mobile  
65 marine weather observations system based on a solar-powered, unmanned vehicle,  
66 named Marine Weather Observer (MWO). To test the observation capability and  
67 endurance, one of the MWOs cruised over the South China Sea from June to August  
68 2020, during which a tropical cyclone formed and turned into a weak typhoon. The  
69 MWO was then remotely controlled to actively approach the center of Typhoon  
70 Sinlaku on August 1st, 2020, providing valuable in-situ observations for typhoon  
71 research and forecasting (Chen et al., 2021, hereafter Chen21).

72 To better understand the quality of observations obtained from MWO, we directly  
73 compared the observations of MWO and several buoys around it over the South China  
74 Sea during the evolutions of Typhoon Sinlaku. The outline of the paper is described

75 below. In Section 2, we briefly describe Typhoon Sinlaku and the observations  
76 obtained from MWO and the buoys. Then MWO observations and the comparisons  
77 with buoys observations are presented in Section 3. The observation difference  
78 between MWO and buoys are discussed in Section 4, and finally a summary is given  
79 in Section 5.

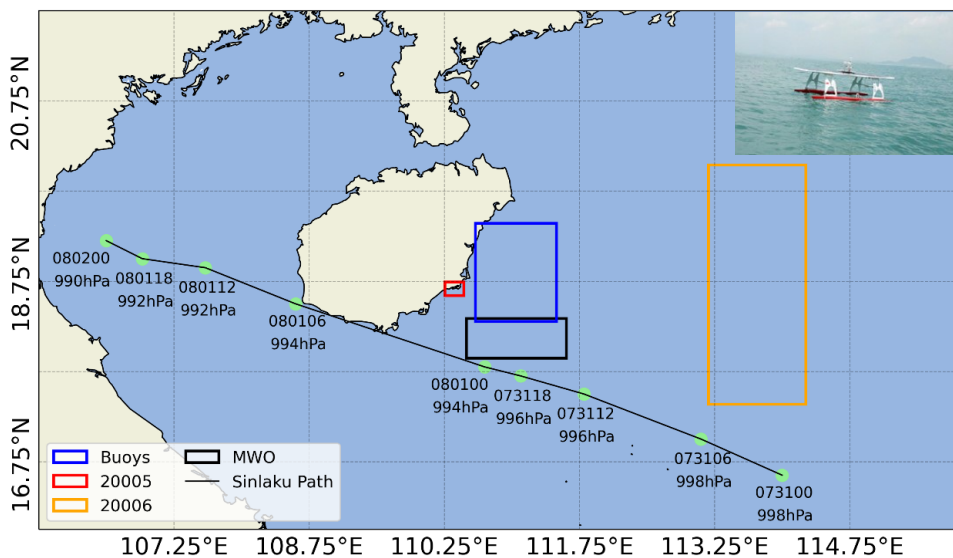
## 80 **2 Typhoon Sinlaku and the related observations**

81 Typhoon Sinlaku (No. 2003) formed as a tropical depression over the South  
82 China Sea on July 31, 2020, then intensified into a typhoon on August 1. The center of  
83 the typhoon crossed Hainan Island, China at a speed of 25 km/h and finally made  
84 landfall off the coast of Thanh Hoa City, Vietnam, at 0840 UTC on August 2.

85 To better monitor the evolution of Typhoon Sinlaku, MWO was used for the first  
86 time to obtain in-situ meteorological observations under extreme sea conditions. The  
87 detailed MWO design and performance were described in Chen21. Measurements of  
88 atmospheric and oceanic environment variables are accomplished with instruments  
89 mounted on MWO, including the AirMar 220WX automatic weather station, mini-CT  
90 sensor, and pyranometer. High temporal resolution (1 minute) data on atmospheric  
91 temperature and humidity, air pressure, wind speed, wind direction, sea surface  
92 temperature (SST), seawater conductivity, and total radiation can be automatically  
93 transmitted to the ground control center via the Beidou communication satellite.  
94 Detailed technical specifications of the meteorological and hydrological sensors can  
95 be found in Chen21.

96 To evaluate the quality of the observations obtained from MWO, we mainly

97 compared them in this paper with the buoy observations conducted simultaneously  
 98 during the typhoon Sinlaku observation experiments from July 22 to August 4 (Zhang  
 99 et al., 2021, Qin et al., 2022). The buoy data consisted mainly of five mooring and two  
 100 drifting buoys that were able to provide the same environmental variables measured  
 101 on MWO from July 23 to August 2 with a 10-minute interval. Thus, the 1-minute  
 102 observations from the MWO were averaged into 10-minute results and then matched  
 103 with the 10-minute observations from the buoys. More than 1300 matched samples at  
 104 10-minute intervals were obtained from July 24 to August 2, 2020, covering the main  
 105 evolution periods of Typhoon Sinlaku in the South China Sea.



106  
 107 Fig.1. Observation ranges of three observation methods, including 5 mooring buoys in the blue  
 108 box, 2 drifting buoys (20005 and 20006), and MWO(as shown in the small photo in the upper right  
 109 corner). The red, orange, and black boxes are the observation ranges of two drifting buoys and MWO  
 110 from July 24 to Aug.2, 2020, respectively. The light green dots marked with date and surface level  
 111 pressure on the black line are the locations of Typhoon Sinlaku from 0000UTC on July 31 to  
 112 0000UTC on August 2, which is from the best track typhoon provided by JMA.

113  
 114 From the locations and the observation ranges of the buoys and MWO in Fig.1, it

115 can be seen that for the two drifting buoys (20005 and 20006, named D05 and D06,  
116 respectively), the drifting range of D05 is very close to the moving area of MWO,  
117 while the drifting path of D06 is about 3-4 degree from MWO in longitude. For the  
118 five mooring buoys in the blue box, one buoy named M64 is the closest, while the  
119 others are located within about 100 km from MWO.

120

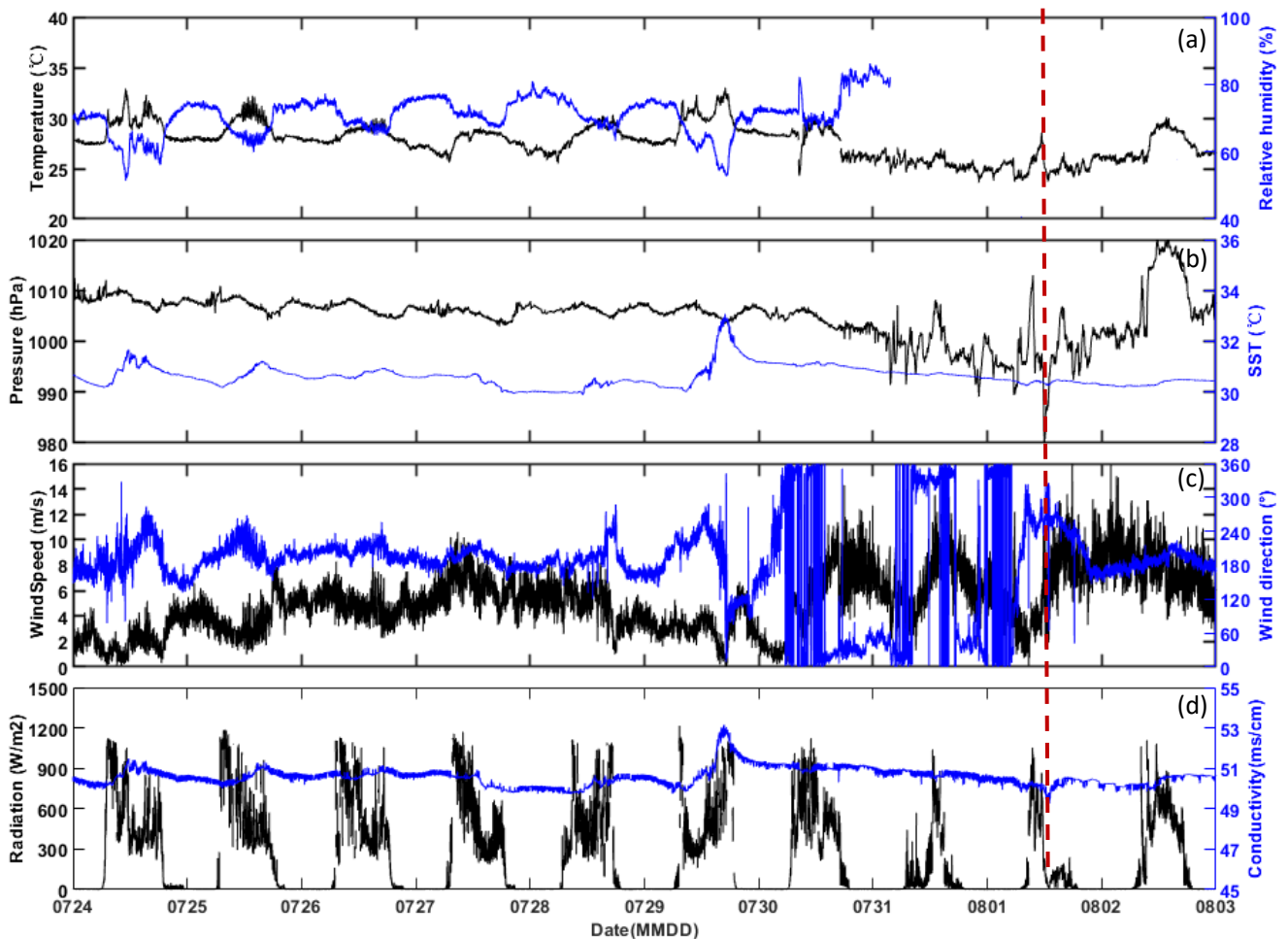
## 121 **3 Results**

### 122 **3.1 The observations from MWO**

123 First, the time series of environmental variables measured by MWO at **1-minute**  
124 interval from July 24 to August 2, 2020 are presented in Fig.2. **It should note that the**  
125 **time used in the following is local time (shorted for LT), also known as Beijing time.** It  
126 can be seen that in the first stage before the arrival of the typhoon, such as July 24-29,  
127 the air temperature and humidity show a clear diurnal variation and negative  
128 correlations, and the air pressure, SST, and seawater conductivity also show small and  
129 stable variation.

130 Then from late July 29 to August 1, the typhoon moved toward the observation  
131 area of MWO. The wind gradually strengthened, and the wind direction frequently  
132 changed from south to north. The air pressure, air temperature, SST, and seawater  
133 conductivity gradually decreased. On July 31, MWO was about 30 km away from  
134 Typhoon Sinlaku and then actively moved to the predicted path of Sinlaku by remote  
135 control. The drastic changes in air pressure and wind speed can be seen around noon  
136 on August 1. Unfortunately, the humidity sensor stopped working on July 31.

137 MWO arrived at the predicted passing area of Sinlaku on August 1st at 09:28,  
 138 with a pressure of 1011 hPa at that time. Then the air pressure decreased to 992 hPa  
 139 around 11:40 and even rapidly dropped to the lowest 980 hPa at 11:58. Subsequently,  
 140 the pressure gradually rose and increased to 992 hPa at 12:56, accompanied by strong  
 141 winds of 15.1 m/s.



142  
 143 **Fig.2.** Time series of (a) air temperature and relative humidity, (b) SST and atmospheric pressure, (c)  
 144 wind speed and direction, and (d) total radiation and seawater conductivity collected onboard MWO  
 145 in the **1-min interval** during the South China Sea typhoon observation experiment from July 24 to  
 146 August 02, 2020. The dashed red line represents the nearest times of MWO passing through the  
 147 typhoon center.

148  
 149 Such drastic fluctuations of air pressure over sea indicated that MWO might be  
 150 cross the typhoon center **around 12 hr on Aug.1**. The subsequent path verification also

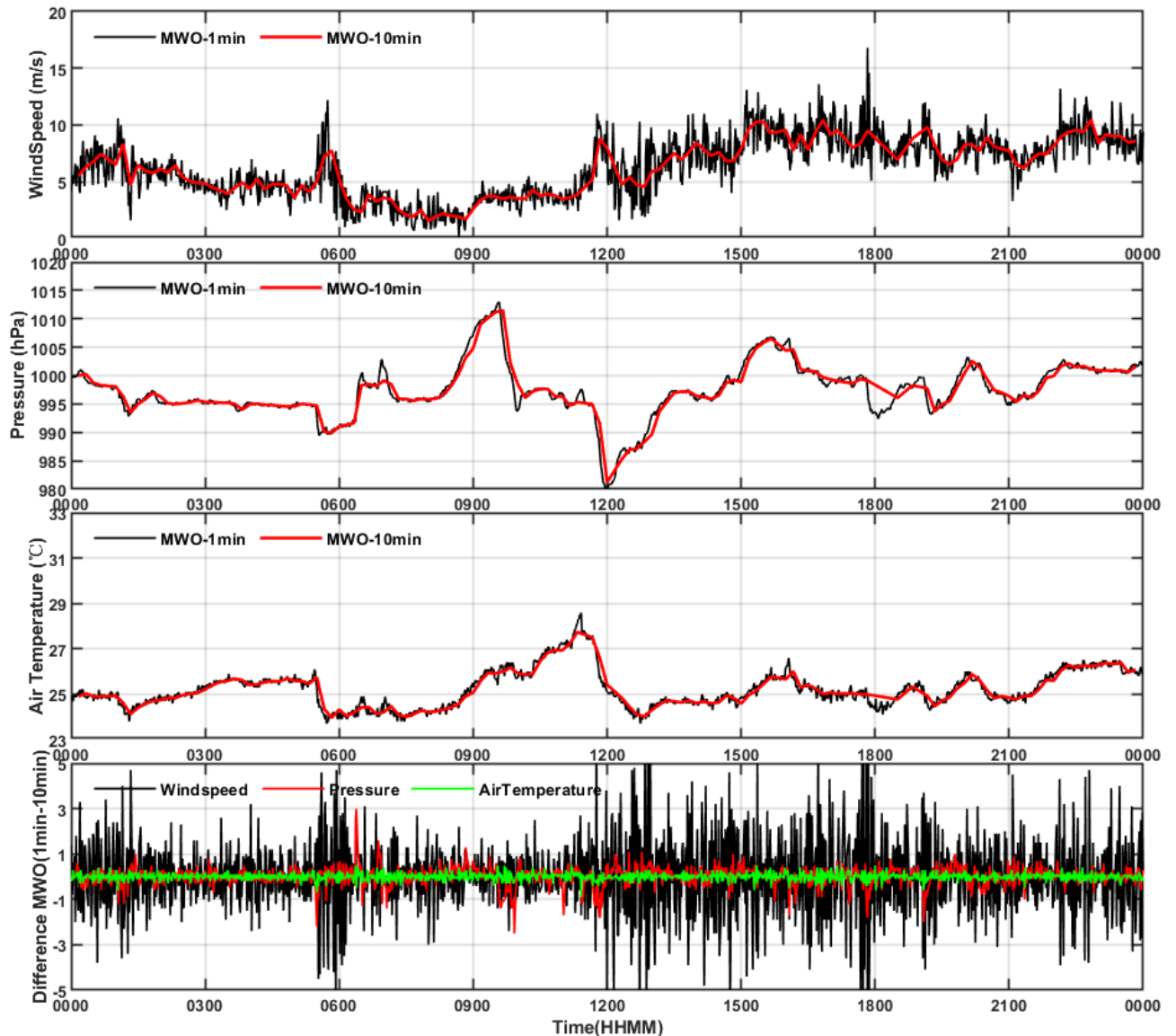
151 proved that MWO was nearly 2.4 km away from the typhoon path issued by the  
152 Central Meteorological Observatory (CMO) of the China Meteorological  
153 Administration, which reflected that MWO successfully passed through the center of  
154 Typhoon Sinlaku. When Sinlaku was moved away from MWO observation range on  
155 August 2, the wind speed gradually decreased and varied less in direction. Compared  
156 with the normal sea conditions in the first stage, we call the next four days (from July  
157 30 to Aug.2) as the second stage with larger changes in sea conditions.

158 To match the 10-minute observations from the buoy, we reprocessed the 1-minute  
159 observations provided by MWO to the 10-minute average. Usually, under stable sea  
160 conditions, the differences in meteorological variables over time may be slight in the  
161 short term. When the typhoon arrived on August 1 and MWO approached the typhoon  
162 center, the variables measured on MWO showed significant changes in Fig. 2.  
163 Therefore, the difference between 1-minute and 10-minute averaged meteorological  
164 variables may be useful for detecting fine-scale structure during typhoons.

165 Thus, the differences between the 1-minute and 10-minute results for the three  
166 variables, including wind speed, air pressure, and air temperature on August 1 are  
167 shown in Fig.3. It is clear that the trends in air pressure (Fig.3b) are consistent for both  
168 time windows, for example, there are two peaks from 06 hr to 10 hr and a sharp drop  
169 to 980 hPa around 12 hr. The air temperature in Fig.3c also shows a highly consistent  
170 variation in the 1-min and 10-min results. However, there is a significant difference in  
171 the wind speed between the two time windows (Fig. 3a). Before 12 hr, both wind  
172 speeds are close to each other and are relatively consistent. As the MWO approaches



173 the typhoon center after 12 hr, the 1-minute wind speed varies more significantly than  
174 the 10-minute wind speed until 18 hr. it is assumed that the 10-minute window may  
175 reflect the average state of the wind field to some extent. the significant difference  
176 between the 1-minute and 10-minute wind speeds reflects the changes in the fine-scale  
177 structure of the wind field during the typhoon evolution. As shown in Fig. 3d, the  
178 differences in pressure and temperature in the two time windows were mostly close to  
179 zero and did not vary much throughout the day on August 1. In contrast, the wind  
180 speed varies greatly with different time interval during most of the day, especially  
181 around 06 hr and 12-18 hr, where the wind speed difference is as high as 5 m/s. This  
182 also reflects the apparent fluctuating behavior of the 1-minute wind field, indicating  
183 strong turbulent activity in the near-surface atmosphere. There has been a lot of  
184 research work on horizontal roll and tornado-scale vortices of typhoons, which are  
185 closely related to the drastic changes in the wind field (Morrison et al. 2005; Lorsolo  
186 et al. 2008; Wurman and Kosiba 2018; Wu et al. 2020). Most of the previous work has  
187 been based mainly on landfalling hurricanes observed by Doppler radar deployed near  
188 the coast. In this work, in situ observations of MWOs that can actively cross typhoon  
189 centers in distant oceanic regions will provide a new perspective to study the fine  
190 structural changes during typhoon evolution.



191

192 Fig.3 The difference between 1-min and 10-min results for wind speed, air pressure, and temperature  
 193 on Aug.1.

194

### 195 3.2 Comparisons of the observations between MWO and buoys

196

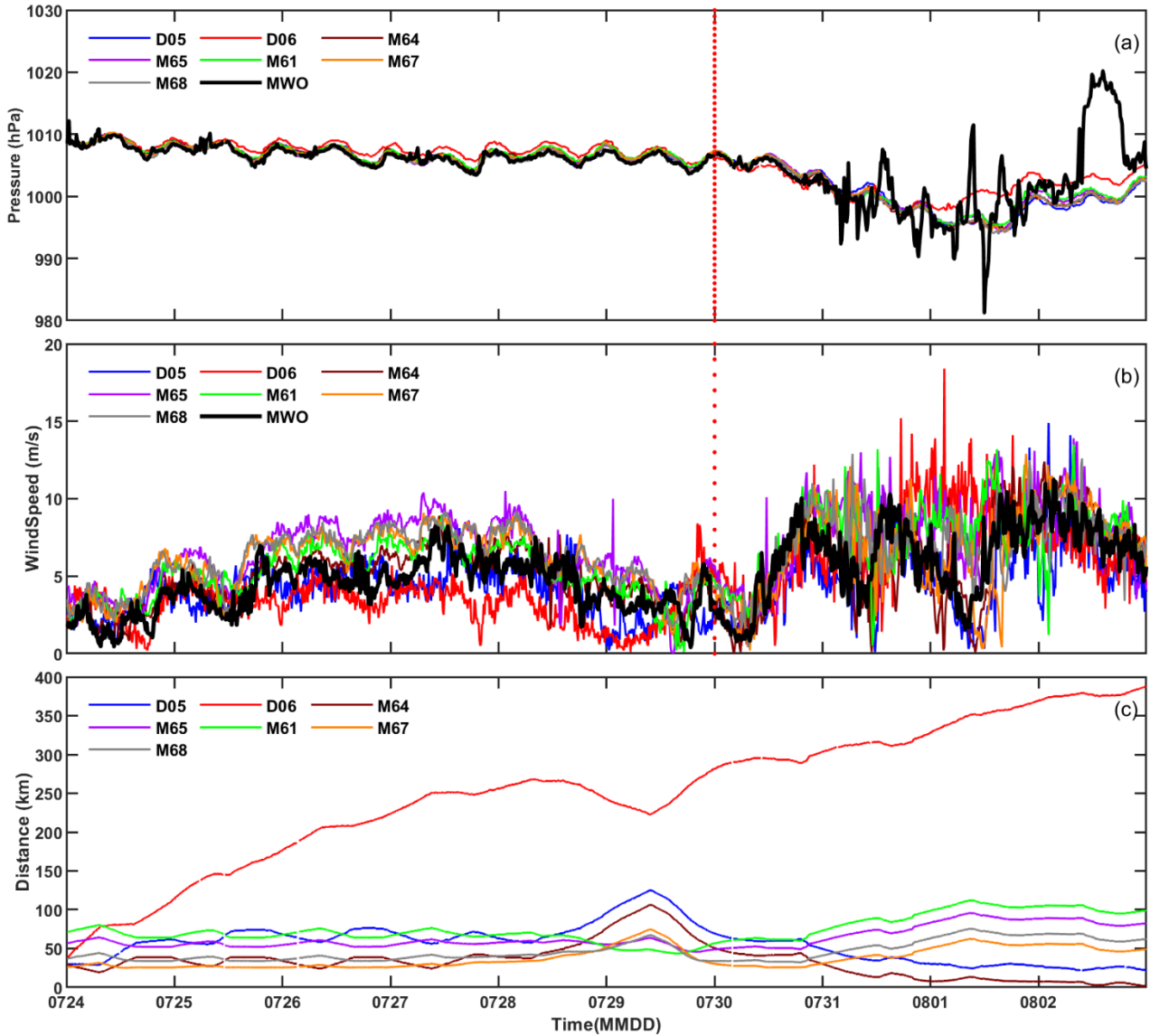
197 To assess the quality of MWO observations, we first compared the air pressure  
 198 and wind speed measured by MWO and all buoys (drifting and moored) as shown in  
 199 Fig. 4. Before seeing the differences in the observations, it is best to know the spatial  
 200 distance variation between MWO and the buoys as shown in Fig. 4c. For the two  
 drifting buoys, the D05 was always closer to the MWO, within 100 km, from July 24

201 to August 2. While D06 gradually moved away from MWO over time, from less than  
202 100 km on July 24 to 400 km on August 2. For the five mooring buoys, M64 is less  
203 than 50 km from MWO from July 24 to 31 and very close to MWO from August 1 to 2.  
204 The rest of the buoys are within 100 km from MWO.

205 Then for the air pressure comparison in Fig. 4a, all buoys and the MWO  
206 measurements in the first stage match very well and basically overlap, except for a  
207 slight difference in the farthest D06. With the arrival of the typhoon, the measured  
208 pressure from MWO changed more obviously, especially around 12 hr on August 1 the  
209 lowest pressure was about 980 hPa when MWO was close to the typhoon center. In  
210 addition, an abnormally high pressure was measured on MWO at 14 hr on August 2,  
211 and the cause of the abnormality is unknown at present. The pressure measured by the  
212 buoys was relatively close and consistent throughout the period, except for a slight  
213 change in the farthest buoy D06.

214 The wind speeds measured from buoys and MWO (Fig.4b) have a good  
215 consistency. They are very close to each other in the first stage due to stable sea  
216 conditions, especially the closer buoys D05 and M64. In the second stage, especially  
217 from July 31 to August 1, there are enhanced changes in wind speed due to the passing  
218 of the typhoon. In the first half of August 1st, there was a significant trend difference  
219 in wind speed from MWO and buoys, for example, the former gradually decreased and  
220 reached its minimum value when MWO is closing to the typhoon center about 12 hr,  
221 while the latter mostly increased during this period. Subsequently, in the second half  
222 of August 1st, the wind speed from MWO rapidly increases to 10m/s, more consistent

223 with those measured from buoys and almost superimposed. As the typhoon gradually  
 224 moved away from the observation domain of MWO and buoys on Aug.2, all wind  
 225 speeds became closer and gradually decreased, returning to the first stage state.



226  
 227 **Fig.4.** Time series of (a) air pressure and (b) wind speed (c) distance for the seven buoys (2 drifting  
 228 and 5 mooring, legend begin with D and M, respectively) and MWO from July 24 to August 02,  
 229 2020. The dashed red line is on July 30 to separate the first and second stages.  
 230

231 Similarly, air temperature and SST obtained from MWO and buoys are compared  
 232 in Fig.5. It seems in Fig.5a that air temperature from MWO is generally lower than  
 233 those from buoys most of the time, especially during the night of the first stage and

234 when approaching the center of the typhoon in the second stage. The diurnal variations  
235 of air temperature measured from MWO and the drifting buoy D05 are more  
236 significant and close in the first stage. Relatively, the air temperature differences  
237 among the mooring buoys are smaller and more stable in the first stage, then enhanced  
238 due to the coming of the typhoon.

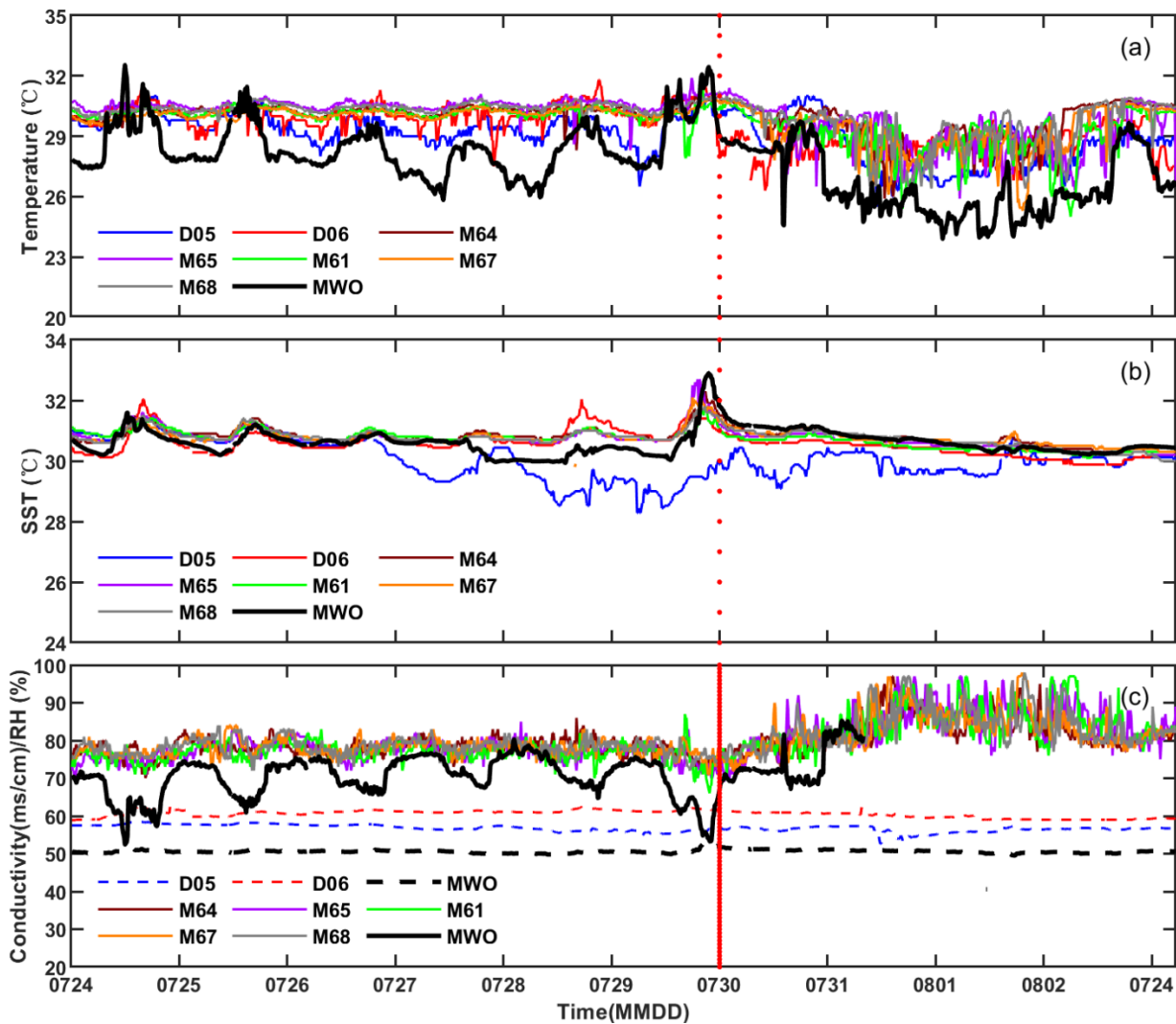
239 For SST shown in Fig.5b, the observations from MWO during the entire period  
240 are very close to those from the five mooring buoys, and are more consistent, even  
241 showing peak areas simultaneously, except for the slight difference from July 27-29.  
242 For the two drifting buoys, the SST measured by the D05 buoy is 1-2 °C lower than  
243 that measured by MWO on July 27-30, while SST measured by the D06 buoy is more  
244 stable and close to that measured by MWO.

245 In addition, seawater conductivity and relative humidity (RH) can be obtained  
246 from MWO. However, only the two drifting buoys can provide seawater conductivity  
247 measurement, and the mooring buoys can provide relative humidity (RH)  
248 measurement. Hence, the seawater conductivity and RH measured from MWO are  
249 compared with those from the corresponding available buoys and displayed in Fig.5c.

250 Firstly, the seawater conductivity measured on MWO and two drifting buoys are  
251 very different, but the detailed values of each instrument are constant throughout the  
252 entire period. The conductivity measurement from D06 buoy is the highest, generally  
253 exceeding 60 mscm<sup>-1</sup>, followed by D05 buoy, which is basically around 57 mscm<sup>-1</sup>,  
254 and the lowest is about 50 mscm<sup>-1</sup> from MWO.

255 The RH difference between mooring buoys and MWO shown in Fig.5c is only

256 available in the first stage because the humidity sensor on MWO stopped working  
 257 after July 30. The RH variations are similar to those of air temperature, that is, RH  
 258 from MWO is mostly lower than that from mooring buoy, especially in the daytime.  
 259 The diurnal variations of RH measured from MWO are more significant while RH  
 260 differences among the mooring buoys are smaller and stable in the first stage.

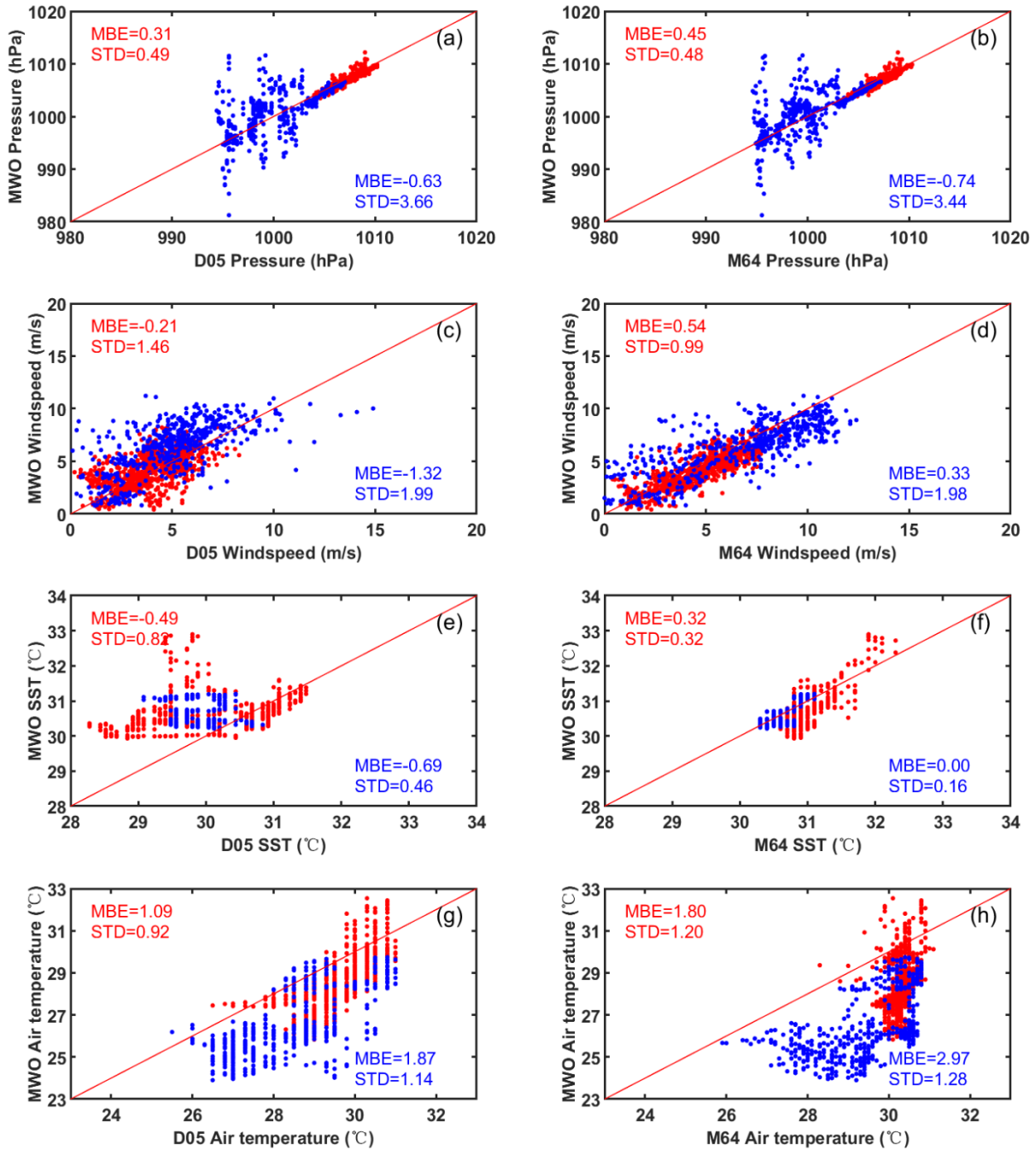


261  
 262 **Fig.5.** Same as Fig.3, except for (a) air temperature, (b) SST, and (c) seawater conductivity (dotted  
 263 line) for drifting buoys and RH (solid line) for the mooring buoys.

264  
 265 To better see the influence of typhoon moving on MWO observations, Fig.6  
 266 shows the scattering plots of meteorological variables observed by MWO and the

267 nearest buoys, including the drifting D05 and the mooring M94. The color samples  
268 and their corresponding statistical results are used to quantify the observations  
269 differences before (in red) and after the arrival of typhoons (in blue). Firstly, before the  
270 arrival of the typhoon, air pressure differences between MWO and both buoys are in  
271 good agreement, as shown in the red samples in Fig.6a,b. Both air pressure differences  
272 are very close and smaller, such as mean bias error (MBE) and standard deviation  
273 (STD) less than 0.5 hPa. However, in the second stage, the pressure difference is  
274 significantly enhanced when MWO approaches the center of the typhoon, shown as  
275 the highly scattered blue samples in Fig. 6a, b, with corresponding STD up to 3.5 hPa.

276 The wind speed measurements from both buoys and MWO have good  
277 consistency in both stages, which is reflected in the good overlap of the red and blue  
278 samples in Fig.6c,d, and the corresponding MBE and STD are very close. For SST  
279 shown in Fig.6e,f, it is seen that the observations between MWO and the mooring  
280 M64 buoy are quite consistent with a difference of less than 0.3°C before and after the  
281 coming of the typhoon. The SST measurements from the drifting buoy D05 are more  
282 scattering with those from MWO the most of time, especially significantly decreased  
283 by about 1-2 °C from July 27 to Aug. 1<sup>st</sup> as shown in Fig.5b. The overall MBE and  
284 STD of SST difference are less than 1.0 °C due to partial overlap of the samples.



285

286

287

288

289

290

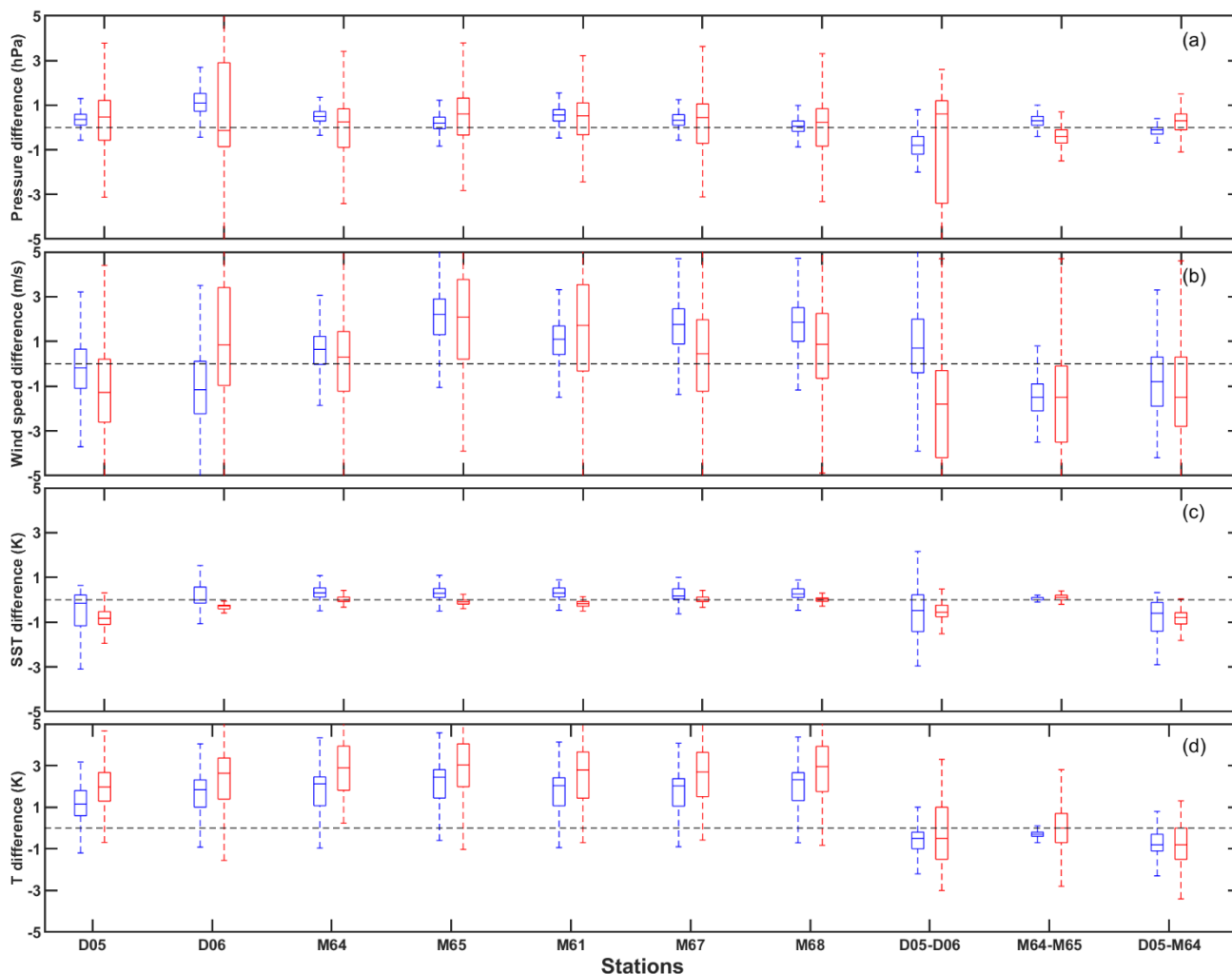
291

Fig.6 Scattering plots of observations from the nearest buoys and MWO, with the drifting D05 in the left column and the mooring M64 in the right column. From top to bottom, they are air pressure, wind speed, SST, and air temperature, respectively.

Regarding air temperature, the observations from MWO show significant fluctuations, while the mooring M64 shown in Fig.6h mostly fixes around 30°C in the first stage. In the second stage, the air temperature measured from MWO is lower than



292 that measured from both buoys, for example, the MBE corresponding to buoys D05  
 293 and M64 is close to  $1.9^{\circ}\text{C}$  and  $3^{\circ}\text{C}$ , respectively. Relatively, the changed trends of air  
 294 temperature measured from MWO and D05 have good consistency in both stages.



295  
 296 Fig.7. The boxplots of observations difference (blue: the first stage; red: the second stage) between  
 297 MWO and seven buoys, as well as between buoys (i.e., D05 and D06, M64 and M65, D05 and M64).  
 298 The observations from up to bottom are air pressure (a), wind speed(b), SST (c), and air temperature  
 299 (d). The dotted line is zero-value line.

300

301 To better understand the observed differences between MWO and buoys, as well  
 302 as between buoys, the boxplots in Fig. 7 show the distribution of their differences in  
 303 pressure, wind speed, SST, and air temperature during the first (blue) and second (red)  
 304 stages. The center marker in each box indicates the median, and the bottom and top

305 edges of the box indicate the 25th and 75th percentiles, respectively. The first seven  
306 buoys reflect the difference between the buoy observations and MWO observations.  
307 The last three reflect differences in observations between buoys, including the two  
308 drifting buoys D05 and D06, the nearest (M64) and farthest mooring buoys(M65)  
309 from the MWO, and the nearest drifting D05 and moored M64 from the MWO.

310 The pressure difference in Fig. 7a shows a clear change in the first and second  
311 stage. Before the arrival of the typhoon, the pressure difference between MWO and  
312 the buoys are close to zero, and the magnitude of the differences between MWO and  
313 the buoys vary relatively uniformly, indicating that the pressure measured by MWO  
314 has the same level of accuracy as those measured by buoys under normal sea  
315 conditions. In the second stage, the range of pressure difference between MWO and  
316 buoy is 2-3 times larger than that in the first stage, but the median value of pressure  
317 difference is still relatively close, mostly within 1hPa. Relatively, the pressure  
318 differences between the buoys in both stages are relatively small and stable, except for  
319 the farthest D06.

320 The median difference of wind speed between MWO and the buoys are mostly  
321 within 1 m/s as shown in Fig. 7b. The wind speed difference in the second stage is  
322 significantly larger than that in the first stage. The wind speed difference between  
323 buoys seems to increase with the distance between buoys, as in the more distant buoys  
324 D06 and M65. In general, the wind speed differences between MWO and buoys are  
325 comparable to the wind speed differences between buoys.

326 For the SST in Fig. 7c, the observed differences between MWO and the moored

327 buoys are very small throughout the period and even better in the second stage. In  
328 contrast, the difference in SST between MWO and the two drifting buoys is not as  
329 good as that between the moored buoys, especially for the closest buoy, D05, which  
330 fluctuates more in the first period, which may indicate that the SST quality of D05  
331 buoy is not as good as its other measurements, such as pressure and wind speed.

332 The difference in air temperature between MWO and the buoys (Fig. 7d) is more  
333 pronounced than the difference in SST. Because of the lower temperature measured by  
334 MWO, the median of temperature difference with the buoys is mostly positive, e.g., 1  
335 K in the first stage and 2 K in the second stage, while the temperature difference  
336 between the buoys is smaller in the first stage and increases significantly by a factor of  
337 2-3 in the second stage.

#### 338 **4 Discussions**

339 In this paper, we first used 1-minute MWO in-situ observation data to monitor the  
340 changes in air pressure, wind field, temperature, and humidity before and after the  
341 arrival of typhoons. In particular, the air pressure significantly decreased from 1010  
342 hPa under normal sea conditions to 980 hPa at the time when MWO crossed the center  
343 of the typhoon. During this period the air pressure underwent obvious and detailed  
344 fluctuations, which cannot be provided by previous observations. In addition, the wind  
345 field reflected the detailed and obvious fluctuations when the typhoon approached.  
346 The air temperature and relative humidity in the lower layers of the sea exhibited  
347 obvious diurnal variations. In contrast, SST is more stable, showing slight changes  
348 before and after the typhoon.

349 Further comparison with buoys observations during the same period revealed that  
350 under normal sea conditions before the arrival of the typhoon, the air pressure and  
351 wind speed measured by MWO and buoys showed good consistency, especially the  
352 difference in air pressure was only less than 0.5 hPa, and the wind speed difference  
353 was less than 0.5 m/s. Moreover, the difference between MWO and buoys was  
354 comparable to that of multiple buoys, indicating that the measurement accuracy of air  
355 pressure and wind speed on MWO was equivalent to that of the buoys under normal  
356 sea conditions. With the arrival of the typhoon, the air pressure measured on MWO  
357 fluctuated greatly, while the corresponding measurements on the buoys were more  
358 stable, resulting in a significant pressure difference between MWO and the buoys.  
359 This may mainly be related to the location where MWO crossed the center of the  
360 typhoon. In addition, as the typhoon departed, the air pressure and temperature  
361 measured on MWO showed abnormally high values around 14 hr on August 2nd, and  
362 then returned to normal range at night, which may be related to unknown external  
363 interference.

364 The trend of wind speed change between MWO and the buoys was more  
365 consistent before and after the arrival of the typhoon. When MWO was closest to the  
366 center of the typhoon, the wind speed change between MWO and the buoys was  
367 slightly misaligned.

368 For the air temperature and relative humidity under normal sea conditions,  
369 measurements made by the mooring buoys were relatively constant and little  
370 variations in a day; the corresponding drifting buoys measurements showed weak

371 diurnal fluctuations; MWO measurements fluctuated significantly from day to night.  
372 This may be related to the installation height and sensitivity of sensors. Usually, the  
373 sensor on the mooring buoy can reach up to 10m, on the drifting buoy and MWO it  
374 may be about 1.0m (Cao et al.,2019). The closer the sensor is to the surface, the more  
375 pronounced the impact of near-surface environmental changes.

376 Compared with other variables, the SST variation before and after the typhoon's  
377 arrival was weak and appeared relatively stable. In particular, the SST measurements  
378 from MWO and the mooring buoys were very close throughout the period. However,  
379 the larger difference in SST between MWO and the nearest drifting buoy may be  
380 caused by the quality of the SST measurement from the latter.

## 381 **5 Summary**

382 During the typhoon observation experiment in the South China Sea in  
383 July-August 2020, MWO completed long-term continuous observations, especially by  
384 actively approaching the center of Typhoon Sinlaku in the deep sea. The in-situ  
385 meteorological and hydrological observations obtained by MWO were evaluated by  
386 comparing them with the observations made by two types of buoys during the  
387 evolution of Typhoon Sinlaku. We obtained some preliminary results as follows.

388 1) Before the arrival of the typhoon, air pressure and wind speed measured by  
389 MWO and the buoys were in good agreement, with the difference in air pressure less  
390 than 0.5hPa and the difference in wind speed less than 0.5 m/s, indicating that the  
391 measurement accuracy of air pressure and wind speed obtained by the two methods is  
392 comparable under normal sea conditions.

393 2) The SST observations of MWO and the mooring buoys show highly consistent  
394 in the entire period, demonstrating the high stability and accuracy of SST  
395 measurements from MWO during the typhoon evolution.

396 3) The air temperature and relative humidity measured from MWO have obvious  
397 diurnal variations and are generally lower than those from the buoys, which may be  
398 related to the mounting height and sensitivity of sensors.

399 4) When actively approaching the typhoon center, the air pressure measured by  
400 MWO can reflect some drastic and subtle changes, such as a sudden drop to 980 hPa,  
401 which is difficult to obtain by other observation methods.

402 As a mobile meteorological and oceanographic observation station, MWO has  
403 shown its unique advantages over traditional observation methods. Although we only  
404 analyzed and evaluated the in-situ observations obtained in one individual case of  
405 MWO crossing the Typhoon Sinlaku in this paper, the results preliminary demonstrate  
406 the reliable observation capability of MWO. For better monitoring of typhoon systems,  
407 it will be necessary to deploy a meteorological and hydrological observation network  
408 composed of multiple MWOs in the future, which will provide comprehensive in-situ  
409 observations on spatial and temporal scales required for forecasting, warnings, and  
410 research of marine meteorological hazards.

411 ***Acknowledgments.*** This work is supported by the National Natural Science  
412 Foundation of China (Grant No. 41627808), the Key Technologies Research and  
413 Development Program (Grant No. 2018YFC1506401), the Shanghai Typhon Reseach  
414 Foundation (Grant No. TFJJ202101). We wish to express our sincere gratitude to

415 Beijing Chunyi Aviation Technology Co., Ltd., Hainan Meteorological Service, Wang  
416 Hu, and Wang Chunhua of Qionghai Meteorological Service, and all personnel who  
417 participated in this experiment.

## 418 REFERENCES

- 419 Bell, M. M., Montgomery M. T., and Emanuel K. A.: Air-sea enthalpy and momentum exchange at  
420 major hurricane wind speeds observed during CBLAST, *Journal of Atmospheric Sciences*, 69,  
421 3197–3222, 2012.
- 422 Bender, M. A., Ginis I., Tuleya R., Thomas B., and Marchok T.: The operational GFDL coupled  
423 hurricane-ocean prediction system and a summary of its performance, *Monthly Weather Review*,  
424 135(12), 3965–3989, 2007.
- 425 Black, P. G., and Coauthors: Air-sea exchange in hurricanes: Synthesis of observations from the  
426 coupled boundary layer air-sea transfer experiment, *Bulletin of the American Meteorological  
427 Society*, 88(3), 357–374, 2007.
- 428 Cao X. Z., Li X. X., Lei Y., et al.: Typhoon observation and analysis of domestic marine  
429 meteorological drift buoy experiment, *Meteor Mon*, 45(10):1457-143, 2019 (in Chinese).
- 430 Chen, H. B., Li J., Ma S. Q., Hu S. Z.: Progress of the marine meteorological observation  
431 technologies, *China Association for Science and Technology*, 37, 91-97, 2019.
- 432 Chen. H. B., LI J., He W., Ma S., Wei Y., Pan J., Zhao Y., Zhang X., Hu S.: IAP's solar-powered  
433 unmanned surface vehicle actively passes through the center of Typhoon Sinlaku (2020), *Adv.  
434 Atmos. Sci.*, 38(4), 538–545, 2021.
- 435 Dai, H. L., Mou N. X., Wang C. Y., and Tian M. Y.: Development status and trend of ocean buoy in  
436 China, *Meteorological, Hydrological and Marine Instruments*, 118–121, 125, 2014.
- 437 Emanuel, K., and Center L.: 100 Years of Progress in Tropical Cyclone Research, *Meteorological  
438 Monographs*, 59, 15.1-15.68, 2018
- 439 Ito, K. and Wu C. C.: Typhoon-position-oriented sensitivity analysis. Part I: Theory and verification,  
440 *Journal of Atmospheric Sciences*, 70, 2525-2546, 2013.
- 441 Lei, X. T: Overview of the development of Typhoon scientific research in China in the past century,  
442 *Science China: Earth Sciences*, 50(3), 321-338, 2020.
- 443 Lenan, L. and Melville W.K.: Autonomous surface vehicle measurements of the ocean's response to  
444 tropical cyclone Freda, *Journal of Atmospheric and Oceanic Technology*, 31(10), 2169–2190,  
445 2014.
- 446 Lorsolo, S., Schroeder J. L., Dodge P., and Marks F.: An observational study of hurricane boundary  
447 layer small-scale coherent structures, *Mon. Wea. Rev.*, 136, 2871–2893, 2008.
- 448 Morrison, I., Businger S., Marks F., Dodge P., and Businger J. A.: An observational case for the  
449 prevalence of roll vortices in the hurricane boundary layer, *J. Atmos. Sci.*, 62, 2662–2673, 2005.
- 450 Qin G., Lei Y., Li X., Cao X., Wang Y., Xu M., Zhou W.: Operational assessment of domestic marine  
451 meteorological drifting buoys, *Meteorological Science and Technology*, 50(4), 467-475, 2022.
- 452 Rogers, R., S. Aberson, A. Aksoy, et al.: NOAA's hurricane intensity forecasting experiment: A  
453 progress report, *Bulletin of the American Meteorological Society*, 94, 859-882, 2013.
- 454 Sanford, T. B., Price J. F., Girton J. B., and Webb D. C.: Highly resolved observations and

455 simulations of the ocean response to a hurricane, *Geophysical Research Letters*, 34 (13),  
456 L13604, 2007.

457 Schmidt K.M., Swart S., Reason C., Nicholson S.A.: Evaluation of satellite and reanalysis wind  
458 products with in situ wave glider wind observations in the Southern Ocean, *J Atmos Ocean*  
459 *Technol*, 34:2551–2568, 2017.

460 Thomson, J., and Girton J.: Sustained measurements of Southern Ocean air-sea coupling from a  
461 Wave Glider autonomous surface vehicle. *Oceanography* 30(2):104–109,2017.

462 Wynn, R. B., and Coauthors: Autonomous Underwater Vehicles (AUVs): Their past, present and  
463 future contributions to the advancement of marine geoscience, *Marine Geology*, 352, 451–468,  
464 2014.

465 Xu, X. F, Gu J. F., Li Y. P.: Marine meteorological disaster [M]. Beijing: China Meteorological Press,  
466 1-4,2009.

467 Yang, L., Wang D.X., Huang J. et al.: Toward a mesoscale hydrological and marine meteorological  
468 observation network in the South China Sea, *Bulletin of the American Meteorological Society*,  
469 96(7), 1117–1135, 2015.

470 Yu, M. G.: An introduction to military oceanography [M]. Beijing: The People's Liberation Army  
471 Press, 65-67, 2003.

472 Zhang X , Li L.X., Yang R., et al.:Comprehensive Marine Observing Experiment Based on  
473 High-Altitude Large Unmanned Aerial Vehicle(South China Sea Experiment2020 of the "Petrel  
474 Project"), *Advances in Atmospheric Sciences*, **38**(4), 528–535, 2021.

475 Zheng, G. G, Chen H. B., Bian J. C., et al.: Atmospheric sciences entering the 21st century [M].  
476 Beijing: China Meteorological Press, 21-25, 2008.

477 Wu L.G., Liu Q.Y., Zhou X. Y.:A review on fine-scale structures in tropical cyclone boundary layer,  
478 *Journal of the Meteorological Sciences*, 40(1),1-10, 2020.

479 Wurman J, Kosiba K.:The role of small-scale vortices in enhancing surface winds and damage in  
480 Hurricane Harvey ( 2017), *Mon. Wea. Rev.*, 146, 713-722,2018.